H/V ratio and amplification factor:
a numerical experiment using 2.5D modelling

J. P. Narayan

Department of Earthquake Engineering, Indian Institute of Technology,
Roorkee, India.

This paper presents the H/V ratio peak amplitude and frequency, their correlation with the site frequency and amplification factor, and limitations. The basin-edge and flat-layer models with different types of soils in the surficial layer were simulated using 2.5D (two and half dimensional) modeling. The effects of sediment bedrock velocity contrast on the H/V ratio peak frequency and amplitude, and the sensitivity of the H/V ratio peak to both the S-wave transfer function and the ellipticity of Rayleigh waves at the fundamental frequency were studied. Simulated results revealed that H/V ratio peak frequencies for both the basin-edge and flat-layer models were in good agreement with the soils fundamental frequencies, only when velocity contrast was larger than 3.5. The comparison of H/V ratio peak amplitude and amplification factors indicates that the use of amplitude of H/V ratio as amplification factor of soil/site is not justified because the obtained H/V ratio was not in accordance with the velocity contrast and can have any value independent of soil velocity and was not similar in magnitude for radial and transverse components. Analysis of the H/V ratio and spectral amplitudes of responses of basin-edge and flat-layer models revealed that it was the trapping of waves (body waves or surface waves) which was responsible for the spectral peak in the H/V ratio at the fundamental frequency. It was also concluded that surface waves were generated near the edge of the basin and propagated normal to the edge, towards the basin. The peak amplification factors were found in good agreement with the fundamental frequency of soil beneath respective recording stations.

Keywords: H/V Ratio, amplification factor, 2.5D modeling, basin-edge effects and surface wave generation.

Introduction

The H/V ratio of noise has been providing satisfactory estimates of the fundamental frequency of the soft deposits, even though the theoretical background is not clear and no experimentally based consensus was ever reached. So, there is a strong need for clear assessment of the actual possibilities and limitations of the noise-based site effect estimates. There are two basic expla-

nations associated with the H/V ratio: i) microtremors mainly consist of surface waves and the H/V ratio peak frequency is basically related to the ellipticity of Rayleigh waves, which vanishes at the fundamental frequency of site (Nogoshi and Igarashi, 1971; Horike, 1985; Milana et al., 1996 and Chouet et al., 1998), and ii) the H/V ratio in the peak frequency range is not affected by the fundamental mode of Rayleigh waves and is in direct relationship with the transfer functions of the S-waves (Kanai, 1983 and Nakamura, 1989, 2000). Dravinski et al. (1996) and Coulet and Mora (1998) reported on the basis of numerical simulations that the H/V ratio points out the fundamental frequency of site and fails completely for amplification estimates using very shallow source. Zhao et al. (1998) reported that when velocity contrast is very high, the soil effect is strong enough to surpass every other effect, and surface and/or body waves are trapped and there is conspicuous spectral peak at the fundamental frequency, whatever the origin of the noise waves.

In the present study, deeper source was used in the simulation of basin-edge and flat-layer models in contrast to Dravinski et al. (1996) and Coulet and Mora (1998), which constitutes another step towards the establishment of a theoretical background for H/V ratio and its valid use as an amplification factor. The responses of both the basin-edge and flat-layer models were transformed into frequency domain using Fast Fourier Transform (FFT) in order to study the sediment bedrock velocity contrast on the amplification factor, H/V ratio peak frequency and amplitude as well as the sensitivity of the H/V ratio to both the S-wave transfer function of site and the ellipticity of Rayleigh waves at the fundamental frequency. The basin-edge effect on the surface wave generation was also studied. The response of the flat-layer model without soil in the basin was also simulated to use it as a reference site in the computation of the amplification factor. Vacuum formulation was used at the free surface for stability. Sponge boundary condition was implemented on the model edges to avoid edge reflections (Israeli and Orszag, 1981).

Source implementation and boundary conditions

An algorithm based on second order parsimonious staggered grid finite difference approximation (Luo and Schuster, 1990 and Ohminato and Chouet, 1997) of Takenaka and Kennett's (1996) 2.5-D elastodynamic wave equation was used in the simulations. The configuration for 2.5D wave simulation is achieved when the medium properties vary only in two dimensions and are assumed constant in the third direction, and the source-receivers are confined in the same plane. Narayan (2001) inferred that the 3D and 2.5D radiation patterns using double couple source, corroborate with each other in the xz-plane. An explosive source is of little relevance to earthquake related studies because it cannot explain the observed radiation patterns. Therefore, double couple point shear dislocation source was implemented into the com-

putational grid using moment tensor source formulation (Pitarka, 1999 and Narayan, 2001). The second derivative of convolution of a polynomial window $[1 - (\tau - 1)^2]^3$ and the Gaussian function $\exp[-\alpha(T-T_0)^2]$ was used as an excitation function. Here $\tau = \dfrac{T}{T_0}$, $T = 2T_0 + 1$ is variable whose length is equal to the length of the filter or duration of the wavelet, T_0 is time delay to the central point of the filter, $\alpha = (\pi F_0)^2$, $F_0 = 0.87 \times$ desired dominant frequency. Free surface boundary conditions often require careful consideration in numerical schemes for stability and accuracy. In the present study, vacuum formulation was adopted (V_p – P-wave velocity, V_s – S-wave velocity and ρ – density, all tend to zero) in the region above the free surface. Graves (1996) reported that vacuum formulation is stable for second order schemes and is free from grid dispersion associated with Rayleigh waves propagating horizontally as compared to fourth order VF-04 and VF-024 schemes. Sponge boundary condition, developed by Israeli and Orszag (1981) was implemented on the model edges to avoid the edge reflections.

Simulation of basin-edge and flat-layer models

Two layered basin-edge and flat-layer models were simulated with six types of soils (Soil 'A' to Soil 'F'), to study the H/V ratio peak frequency and amplitude, and amplification factors. Figure 1a shows the north-south cross section of the basin-edge model and its southern edge. The northern basin-edge was assumed to be far away. Further, it was assumed that the southern and northern basin-edges were elongated in the east-west direction. Figure 1b shows the flat-layer model with a horizontal layer having thickness of 140 m above the half space. Ten equidistant (350 m) receivers (R1–R10) were used for simulated recording and their locations are shown in Figure 1. The P- and S-wave velocities, densities, Poisson's ratios and fundamental frequencies of different soils in the upper layer and half space (hard rock) are given in Table 1. In the simulation, positive x-coordinate is pointing in the north direction and positive z-coordinate is pointing vertically downward. The basin-edge and flat-layer models ($17.5 \text{ km} \times 16.5 \text{ km}$) were discritised into square grids of size 35 m. The time step and dominant frequency were taken as 0.004 s and 1.0 Hz respectively. The source with focal mechanism of dip = 45.0°, rake = 90.0° and strike = 60.0° was generated 1.155 km south of the edge of the basin at a depth of 14.0 km.

The responses of basin-edge and flat-layer models with different type of soils were analyzed in time domain, to study the role of basin-edge in generation of surface waves. Figure 2 shows the variation of ground displacement in the radial component at different receivers for soils 'A'–'F'. Strong surface waves caused by basin-edge were recorded just after the arrivals of the incoming S-waves. These surface waves were identified based on very large co-
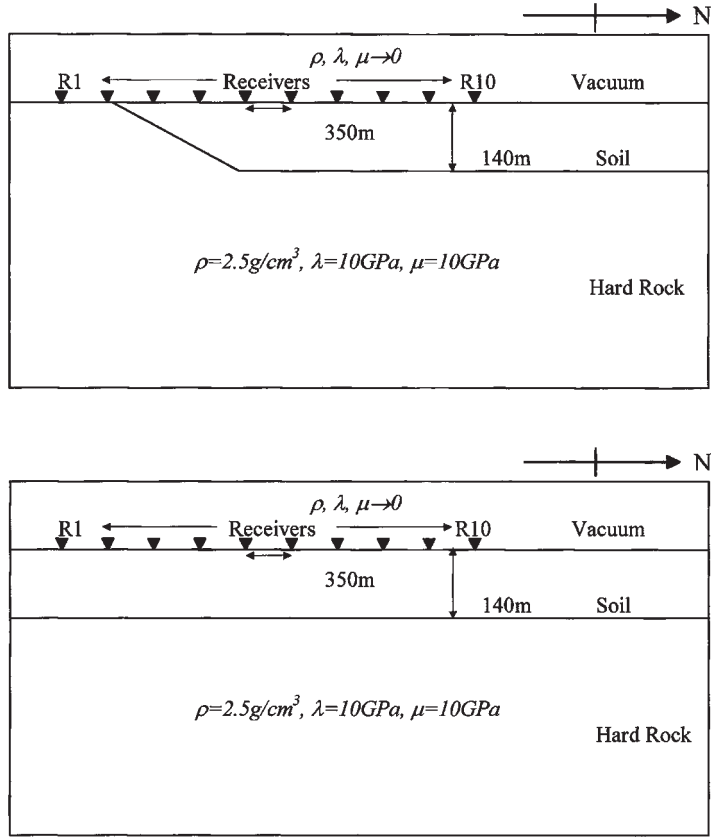
Figure 1. Vertically exaggerated basin-edge (top) and flat-layer (bottom) models and receiver points.

Table 1. Different types of soils and their parameters used in the simulations.

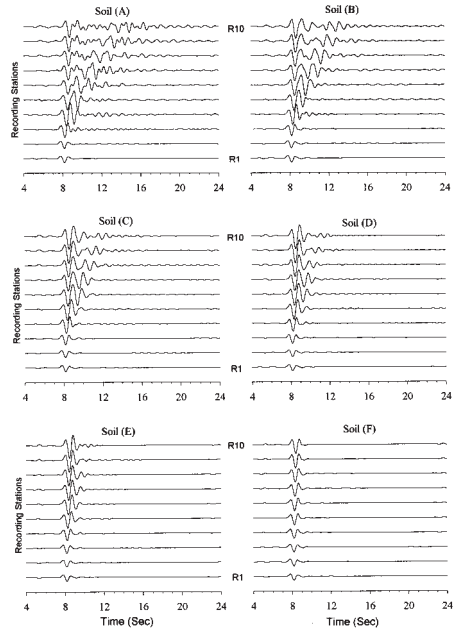| Type of Soil	V_s (m/s)	V_p (m/s)	Density, ρ (g/cm^3)	Poisson's ratio	Thickness of soil, h (m)	Fundamental frequency (Hz)
Soil 'A'	400.00	1800.00	1.90	0.474	140.00	0.714
Soil 'B'	500.00	1900.00	1.95	0.462	140.00	0.892
Soil 'C'	600.00	2000.00	1.95	0.450	140.00	1.071
Soil 'D'	700.00	2100.00	2.10	0.437	140.00	1.250
Soil 'E'	850.00	2200.00	2.15	0.412	140.00	1.517
Soil 'F'	1250.00	2643.00	2.50	0.355	140.00	2.232
Rock	2000.00	3464.10	2.50	0.250	–	–

Figure 2. Radial component of the responses of the basin-edge model with different soils.
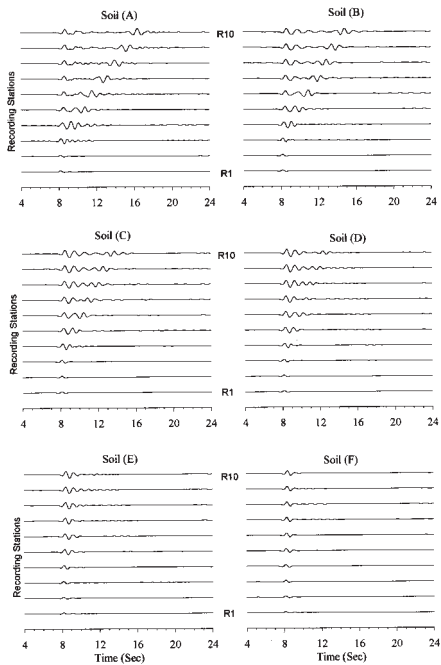

Figure 3. Transverse component of the responses of the basin-edge model with different soils.

herence among the recording stations and the estimated group velocity of the Rayleigh waves. It is clear from the responses that surface waves were generated near the basin-edge and propagated normal to edge, towards the basin. The increase of time separation between the incoming S-waves and the corresponding surface waves, as we go away from the basin-edge confirm the above conclusion. This conclusion gets further support from the decrease of time separation between the S-waves and the corresponding surface waves with the increase of soil velocity in the basin. The amplitude of incoming waves was almost continuously increasing with the decrease of soil velocity in the basin. There was a pronounced increase of surface wave amplitude and duration with the decrease of soil velocity. Large amplitude at stations R4 and R5 may be due to constructive interference of body waves and the surfaces waves. Similar effects on surface wave generation and amplitude amplification in the transverse (Fig. 3) and vertical components (Fig. 4) are observed. In the vertical component (Fig. 4), the amplitudes of surface waves are very large as compared to the incoming waves.

The responses of flat layer model shown in Figure 5 reveal that surface waves were not generated due to deeper focal depth of the source used. The comparison of responses of flat-layer model with basin-edge model reveal that there is almost complete resemblance in the characteristics of incoming waves (body waves), except for minor changes due to the interference and the small thickness of basin-edge. However, there is no similarity in the later arriving phases like multiples and the surface waves. Finally, it is concluded on the basis of comparison of responses of basin-edge and flat-layer models that strong surface waves are generated near the basin edge which propagate normal to the edge towards the basin.

Analysis of H/V ratio and amplification factors

The responses of both the basin-edge and flat-layer models were transformed into frequency domain using Fast Fourier Transform. H/V ratios in the frequency range of 0.2–2.4 Hz were computed at stations R3, R4, R5 and R10, just by dividing the spectra of radial and transverse components by the respective spectra of vertical component. Similarly, the amplification factors of soils were computed by dividing the spectra of radial and transverse components with the respective spectra of the rock site. The response of flat-layer model without soil was considered as the reference at the respective recording station.

Figures 6–9 show the H/V ratios and amplification factors of radial and transverse components corresponding to both the basin-edge and flat-layer models for soils 'A'–'F' at different recording stations. The analysis of these figures reveal that H/V ratio peak frequency for both the radial and transverse components of the basin-edge model at station 'R10' is more or less the
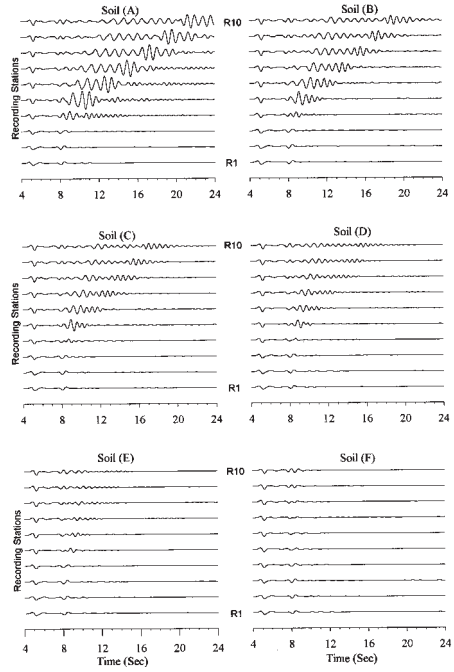
Figure 4. Vertical component of the responses of the basin-edge model with different soils.
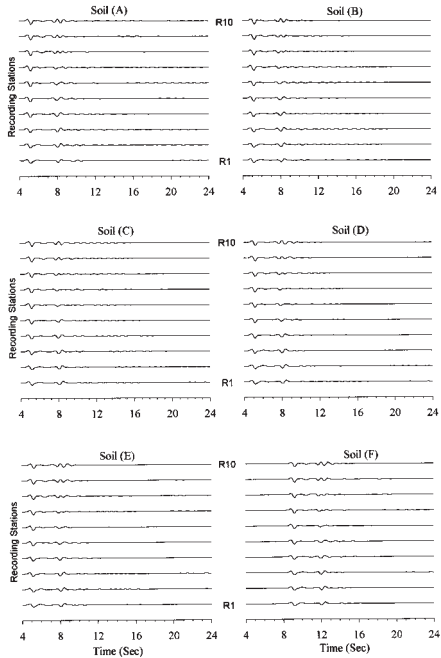

Figure 5. Vertical component of the responses of the flat-layer model with different soils.

same as the fundamental frequency of soils 'A'–'D' (Figs. 6 and 7). This match is not observed for soils 'E' and 'F'. The H/V ratio peak frequency shifts to higher values as we move towards the edge of the basin, but not in a systematic manner as per the velocity and thickness of the soil below the recording site. Similarly, the H/V ratio peak frequencies of flat layer model (Figs. 8 and 9) are almost equal to the fundamental frequencies of the soils 'A'–'C' at all the four receiver points. In case of soil 'D', the H/V ratio peak frequency is in good agreement with the soil fundamental frequency for radial component but not for the transverse component. On the other hand, there is no correlation between the fundamental frequencies of the soils 'E' and 'F' and the respective H/V ratio peak frequency. It is concluded that the H/V ratio peak frequency is in good agreement with the fundamental frequency of soils when the velocity contrast is >3.5. So, to relate the H/V ratio peak frequency only with the horizontal polarization of fundamental mode of Rayleigh waves looks questionable.

Further analysis of Figures 6–9 revealed good agreement between frequency corresponding to peak amplification factor with the fundamental frequency of soils ($V_s/4h$). Figure 6 shows two lobes having high value of amplification factors. The range of frequencies in the first lobe shifts towards the lower value as thickness of soil beneath the recording station increases, according to the fundamental frequency of soil. On the other hand, there is no such shifting of frequency in the second lobe. It means that the amplification factors in the first lobe correspond to the incoming waves and the amplification factors in the second lobe correspond to the surface waves. Similar trend of amplification factor was observed in the transverse component (Fig. 7). The frequency of surface waves is very much dependent on the soil velocity.

The amplification factors are clearly very much in accordance with velocity contrast in both models. However, there is no correlation between the H/V ratio peak amplitude and the amplification factor, even for the very soft soils 'A', 'B' and 'C'. The H/V ratio peak amplitude was very large as compared to the amplification factor at the fundamental frequency. Further, the H/V ratio peak amplitude is not decreasing with the decrease of velocity contrast. The H/V ratio is very low (and even less than one) in contrast to soil to rock spectral ratio in the 0.2–2.4 Hz frequency range. So, the use of amplitude of H/V ratio as amplification factor of soil/site may be dangerous. Since, it was not in accordance with the velocity contrast, it can have any value independent of soil velocity and was not similar in magnitude for radial and transverse components.

The absolute spectral amplitude of the radial, transverse and vertical components of the response of both the basin-edge and flat-layer models for soils 'A', 'B' and 'C' are shown in Figure 10. The analysis of this figure revealed that there was sudden increase in spectral amplitude at the fundamental frequency (Table 1) in the radial and transverse components and sudden drop in the vertical component. So, it is the trapping of wave whether it
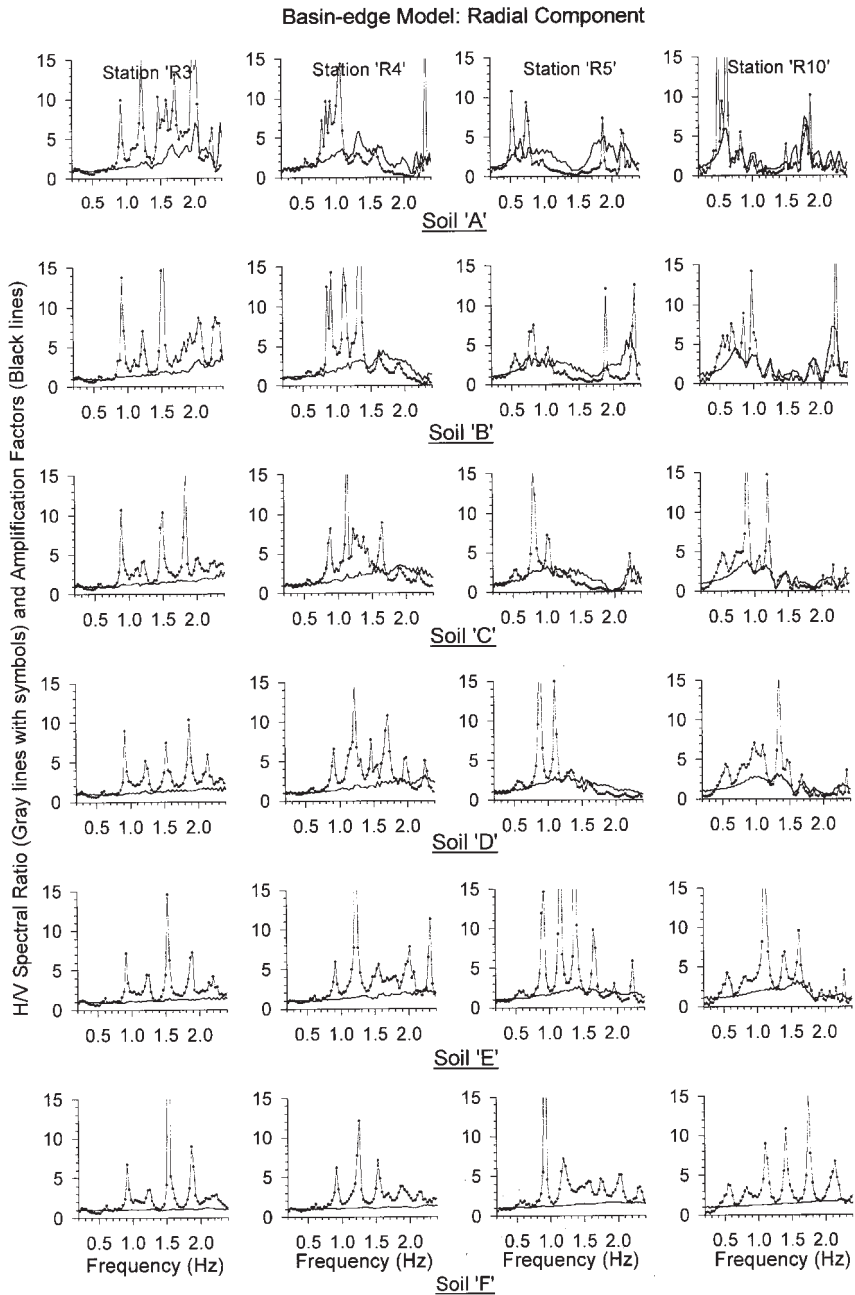
Basin-edge Model: Radial Component

Figure 6. H/V ratio and amplification factors for radial component using different type of soils in the basin-edge model (Note: Gray lines with symbols denote H/V ratio and black lines denote amplification factors).
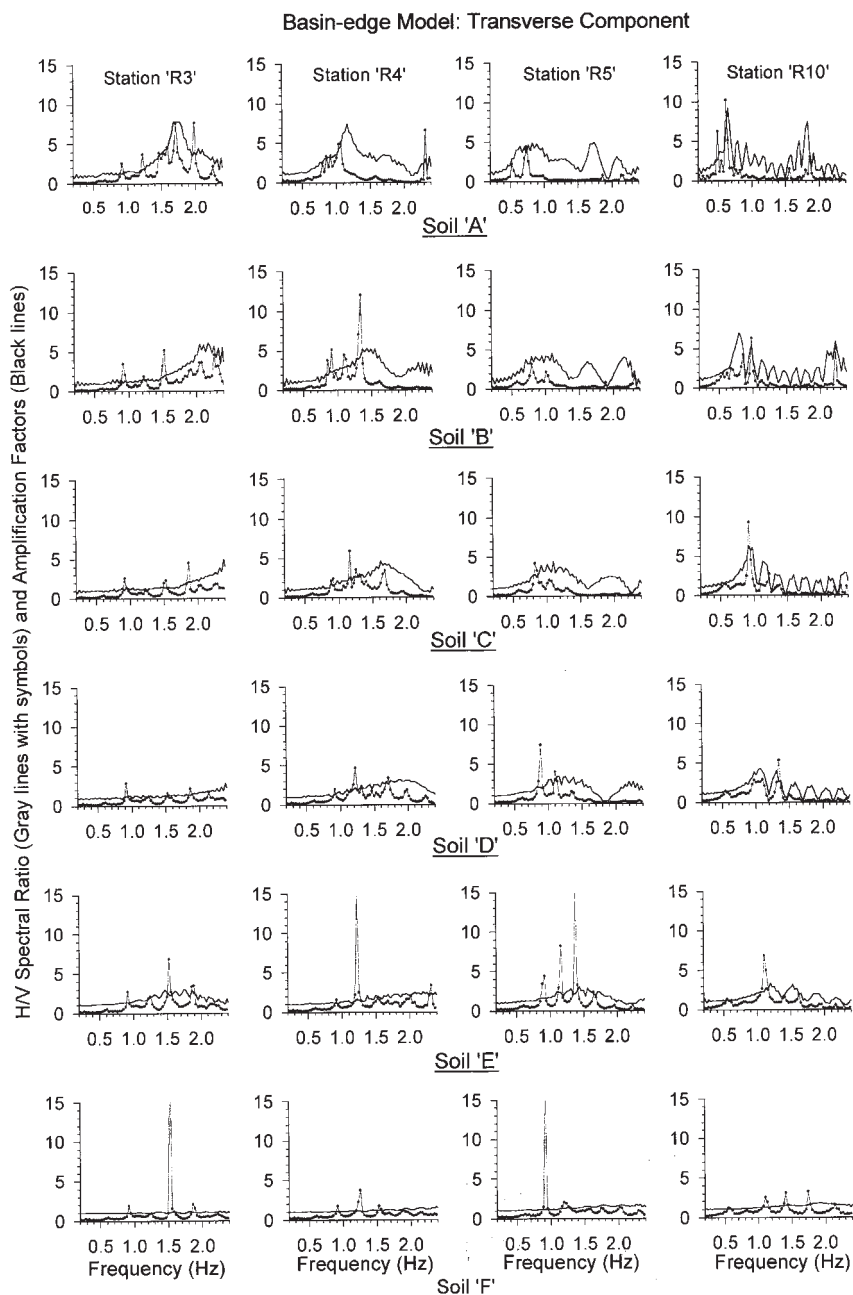
Figure 7. H/V ratio and amplification factors for transverse component using different type of soils in the basin-edge model (Note: Gray lines with symbols denote H/V ratio and black lines denote amplification factors).
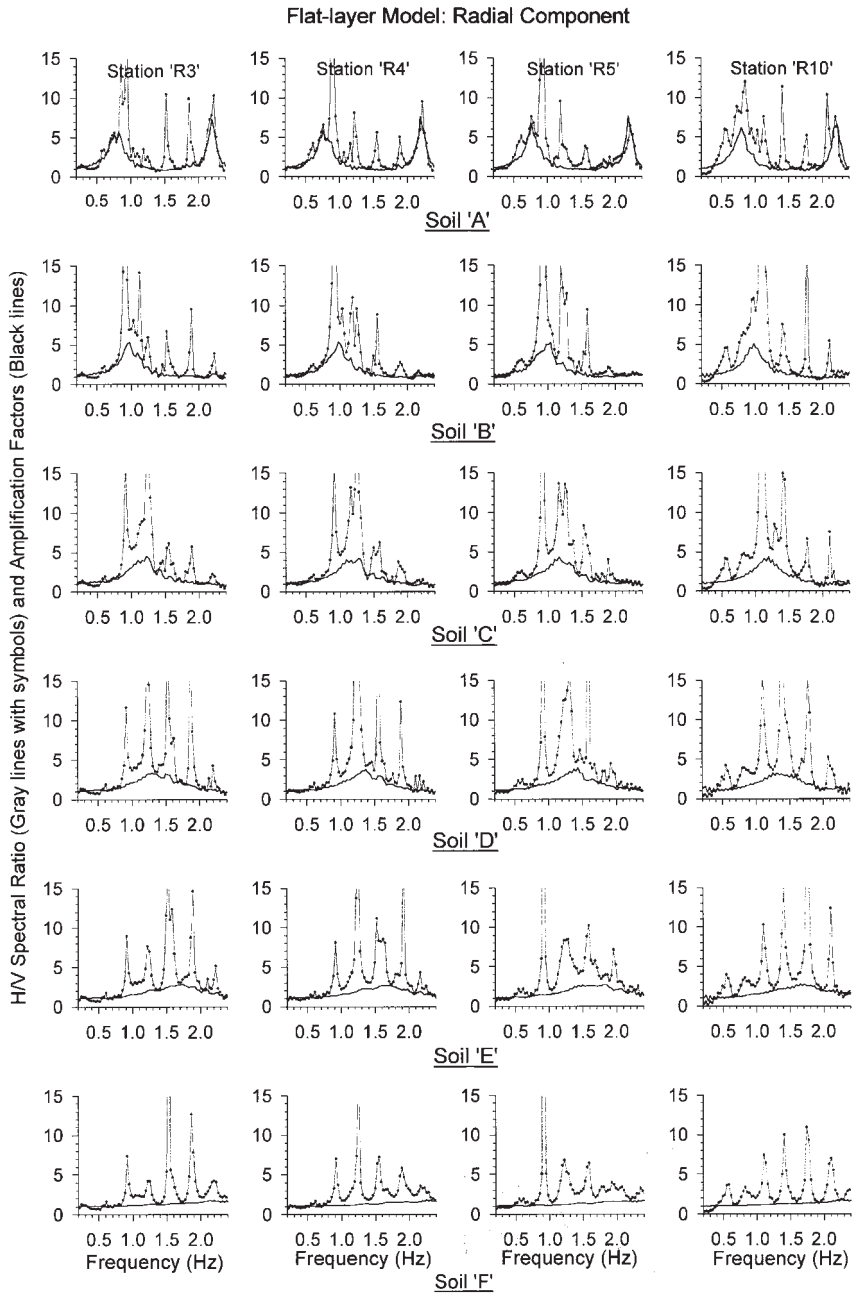
Flat-layer Model: Radial Component

Figure 8. H/V ratio and amplification factors for radial component using different type of soils in the flat-layer model (Note: Gray lines with symbols denote H/V ratio and black lines denote amplification factors).
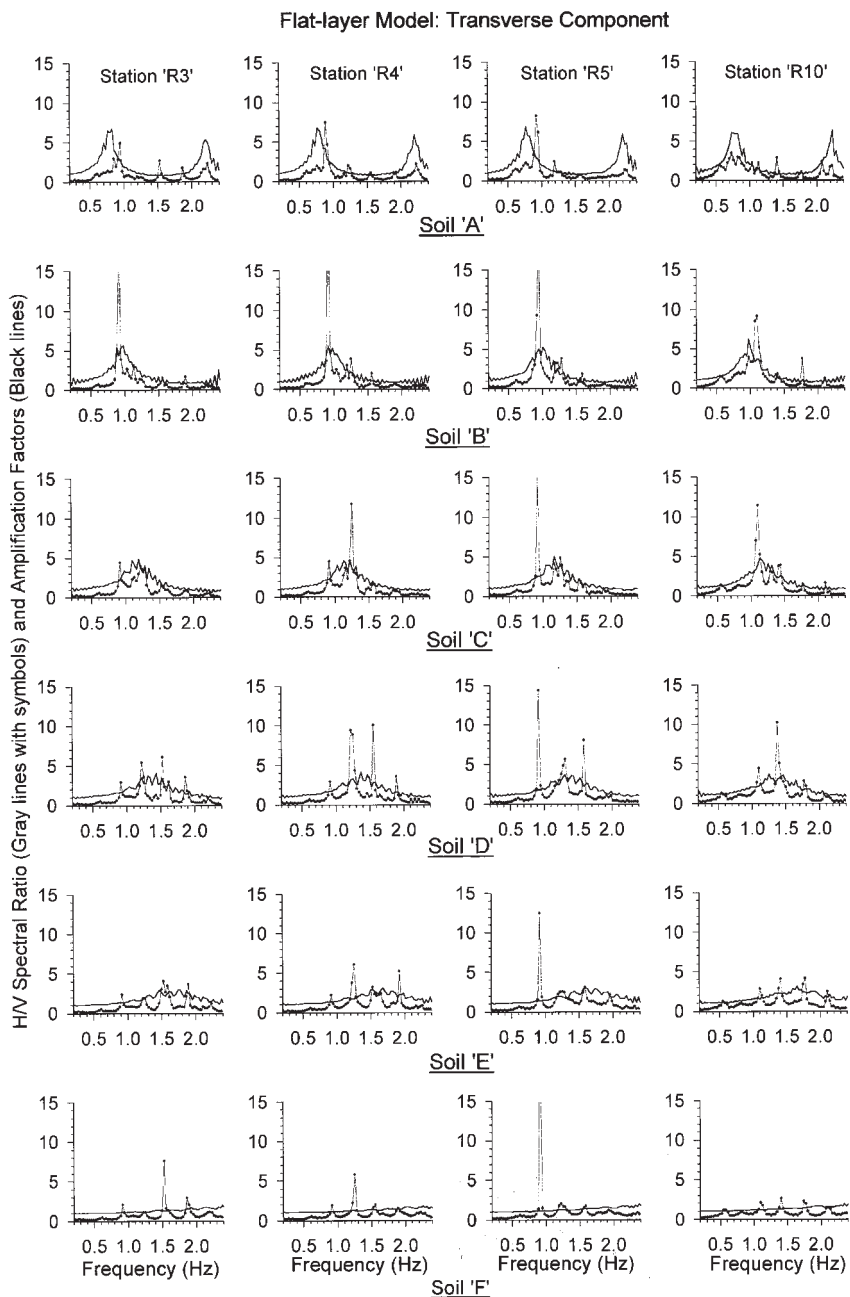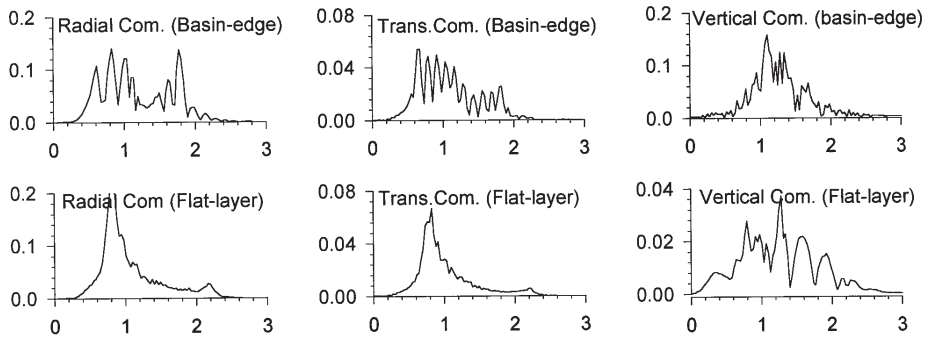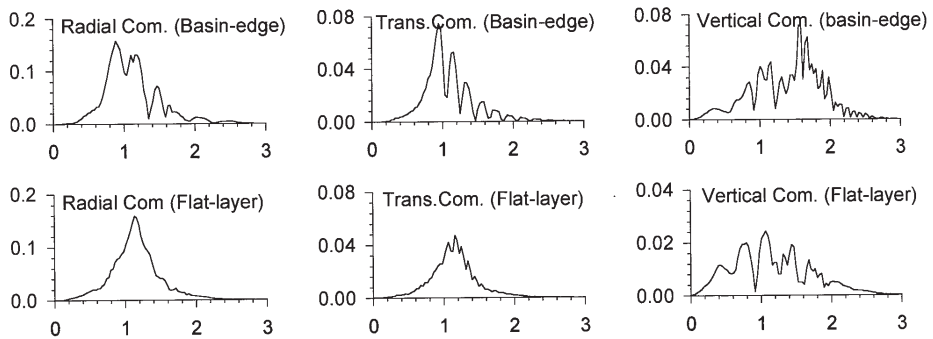
Figure 9. H/V ratio and amplification factors for transverse component caused by different type of soils in the flat-layer model (Note: Gray lines with symbols denote H/V ratio and black lines denote amplification factors).
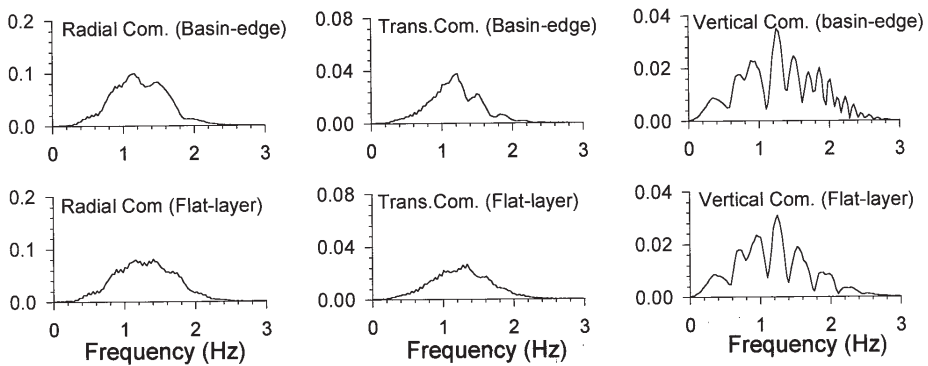
Figure 10. Spectral amplitude for radial, transverse and vertical components of responses of basin-edge and flat-layer models using, a) soil 'A', b) soil 'B' and c) soil 'C'.

is body wave or surface wave which is responsible for the conspicuous spectral peak in the radial and transverse components and trough in the vertical component at the fundamental frequency of soils, finally causing large H/V ratio.

Discussion and conclusions

An algorithm developed by Narayan (2001) using Takenaka and Kennett's (1996) 2.5D elastodynamic wave equation was used in the simulations. In the present study, deeper source than considered by Dravinski et al. (1996) and Coulet and Mora (1998) was used in the simulations of basin-edge and flat layer models so that the physics behind sensitivity of the H/V ratio to S-wave transfer function or the ellipticity of Rayleigh waves at the fundamental frequency could be studied. The simulated results reveal that surface waves are generated near the edge of the basin and propagate towards the basin. Similar conclusion – that later arrival is primarily composed of surface waves generated at the basin-edge (Hatayama et al. 1995; Kawase, 1996 and Pitarka, 1998) – was also drawn in many studies by examining the phase and group velocities, polarity and arrival azimuth (estimated from the later arrivals).

The H/V ratio peak frequencies in both the basin-edge and flat-layer models are in good agreement with the fundamental frequency of the soil, only when velocity contrast is larger than about 3.5. It was concluded that when velocity contrast was very high the soil effect was strong enough to surpass every other effects. The surface and/or body waves are trapped and there is a conspicuous spectral peak in the radial and transverse components and trough in the vertical component at the fundamental frequency. So to relate the H/V ratio peak frequency only with the horizontal polarization of Rayleigh waves at the fundamental frequency is questionable. Similar conclusion was also drawn by Zhao et al. (1998). The trapping of waves, whether they are body waves or surface waves, seems to be responsible for the spectral peak in the H/V ratio at the fundamental frequency.

The analysis of H/V ratio peak amplitude and amplification factors revealed that the H/V ratio is not in accordance with the velocity contrast and is not similar in magnitude in radial and transverse components. Larger as well as smaller values of H/V ratio peak amplitude as compared to amplification factors were also reported by Fischer et al. (1995) and Kanno and Ohmachi (1998). So, it can be concluded that the H/V ratio predicts only fundamental frequency of soft deposits and fails completely for amplification estimates. Similar conclusion was also drawn by Dravinski et al. (1996) and Coulet and Mora (1998), based on numerical simulations.

References

Coulet, F. and Mora, P. (1998): Simulation based comparison of four site-response estimation techniques, Bulletin of the Seismological Society of America, **88**, 30–42.

Chouet, B., Luca, G. De, Milana, G., Dawson, P., Martini, M. and Scarpa, R. (1998): Shallow velocity structure of Stromboli Volcano, Italy, derived from small-aperture array measurements of strombolian tremor, Bulletin of the Seismological Society of America, **88**, 653–666.

Dravinski, M., Ding, G. and Wen, K. L. (1996): Analysis of spectral ratios for estimating ground motion in deep basins, Bulletin of the Seismological Society of America, **86**, 646–654.

Fischer, K. M., Salvati, L. A., Hough, S. E., Gonzalez, E., Nelsen, C. E. and Roth, E. G. (1995): Sediment induced amplification in the Northeastern United States: a case study Providence, Rhode Island, Bulletin of the Seismological Society of America, **85**, 1388–1397.

Graves, R.W. (1996): Simulating seismic wave propagation in 3D elastic media using staggered grid finite difference, Bulletin of the Seismological Society of America, **86**, 1091–1106.

Hatayama, K., Matsunami, K., Iwata, T., and Irikura, K. (1995): Basin-induced Love waves in the eastern part of the Osaka basin. Journal of Physics of the Earth, **43**,131–155.

Horike, M. (1985): Inversion of phase velocity of long-period microtremors to the S-wave velocity structure down to the basement in urbanized areas, Journal of Physics of the Earth, **38**, 59–96.

Israeli, M. and Orszag, S.A. (1981): Approximation of radiation boundary conditions, Journal of Computational Physics, **41**, 115–135.

Kanai, K. (1983): Engineering Seismology, University of Tokyo Press, Tokyo.

Kawase, H. (1996): The cause of damage belt in Kobe: »The basin-edge effect«, constructive interference of the direct S-waves with the basin induced diffracted/Rayleigh waves. Seismological Research Letter, **67**, 25–34.

Konno, K and Ohmachi, T. (1998): ground motion characteristics estimated from spectral ratio between horizontal and vertical components of microtremor, Bulletin of the Seismological Society of America, **88**, 228–241.

Luo, Y. and Schuster, G. (1990): Parsimonious staggered grid finite differencing of the wave equation, Geophysical Research Letter, **17**, 155–158.

Milana, G., Barba, S., Del Pezzo, E. and Zambonelli, E. (1996): Site response from ambient noise measurements: new perspectives from an array study in central Italy, Bulletin of the Seismological Society of America, **86**, 320–328.

Nogoshi, M. and Igarashi, T. (1971): On the amplitude characteristics of microtremor (Part 2), Journal of the Seismological Society of Japan, **24**, 26–40.

Nakamura, Y. (1989): A method for dynamic characteristics estimation of subsurface using microtremore on the ground surface, QR of R.T.R, **30–1**.

Nakamura, Y. (2000): Clear identification of fundamental idea of Nakamura's technique and its applications, Proc. XII World Conference, Earthquake Engineering, New Zealand paper no. **2656**.

Narayan, J. P. (2001): Site-specific strong ground motion prediction using 2.5D modeling, Geophysical Journal International, **146**, 269–281.

Ohminato, T. and Chouet, B. A. (1997): A free surface boundary condition for including 3D topography in the finite difference method, Bulletin of the Seismological Society of America, **87**, 494–515.

Pitarka, A., Irikura, K., Iwata, T., and Sekiguchi, H. (1998): Three dimensional simulation of the near fault ground motion for 1995, Hyogo-ken Nanbu (Kobe), Japan earthquake, Bulletin of the Seismological Society of America, **88**, 428–440.

Pitarka, A. (1999): 3D elastic finite difference modeling of seismic motion using staggered grids with nonuniform spacing, Bulletin of the Seismological Society of America, **89**, 54–68.

Takenaka, H. and Kennett, B. L. N. (1996): A 2.5D time domain elastodynamic equation for plane wave incidence, Geophysical Journal International, **125**, F5–F9.

Zhao, B. M., Horike, M. and Takeuchi, Y. (1998): Reliability of estimation of seismic ground characteristic by microtremor observation, Proceedings of the XIth European Conference on Earthquake Engineering, Paris, Sept. 6–11, Bisch, Labbe & Pecker Editors, Balkema 1998.

SAŽETAK

H/V spektralni omjer i faktor amplifikacije: numerički eksperiment pomoću 2.5-D modeliranja

J. P. Narayan

Razmotren je omjer spektara horizontalne i vertikalne komponente (H/V) gibanja tla, najveća spektralna amplituda i odgovarajuća frekvencija te njihov odnos s karakterističnom frekvencijom i amplifikacijom površinskih slojeva tla. Koristeći 2.5-D modeliranje, simulirani su uvjeti ruba bazena kao i model s horizontalnim sedimentnim slojevima. Proučen je utjecaj kontrasta brzina seizmičkih valova na amplitudu i frekvenciju H/V spektralnog šiljka, kao i njihovu osjetljivost na prijenosnu funkciju S-valova i na eliptičnost Rayleighevih valova u pojedinom modelu. Simulirani rezultati pokazuju da dominantna frekvencija H/V spektra u obje vrste modela odgovara osnovnoj frekvenciji modela samo kad je kontrast brzina između osnovne stijene i slojeva veći od 3.5. Analiza također pokazuje da nije opravdano korištenje H/V spektralnih omjera za procjenu amplifikacijskog spektra, jer nije opažena korelacija između teorijskih amplifikacijskih spektara i simuliranih H/V spektralnih omjera, koji su se čak razlikovali i za radijalnu i transverzalnu horizontalnu komponentu.

Ključne riječi: H/V spektralni smjer, amplifikacija, 2.5-D modeliranje

Corresponding author's address: J. P. Narayan, Department of Earthquake Engineering, Indian Institute of Technology, Roorkee-247667, India, e-mail: jaypnfeq@iitr.ernet.in.